3B2v8.06a/w (Dec 5 2003).51c XML:ver:5.0.1 | MPS : 1178 | Prod.Type:FTP pp.1–30(col.fig.:NIL) | ED:VinuthaM.B. PAGN:Ashok SCAN:Raj

ARTICLE IN PRESS

Available online at www.sciencedirect.com
SCIENCE DIRECT®
Journal of Mechanics and Physics of solids
▮ (▮▮▮▮) ▮▮▮–▮▮▮

ELSEVIER

JOURNAL OF THE MECHANICS AND PHYSICS OF SOLIDS

www.elsevier.com/locate/jmps

Transition waves in bistable structures. II. Analytical solution: wave speed and energy dissipation

Leonid Slepyan[a], Andrej Cherkaev[b,1], Elena Cherkaev[b,*]

[a]*Department of Solid Mechanics, Materials and Systems, Tel Aviv University, Ramat Aviv 69978, Israel*
[b]*Department of Mathematics, The University of Utah, 155 South 1400 East, JWB233, Salt Lake City, UT 84112, USA*

Received 30 January 2004; received in revised form 2 August 2004; accepted 7 August 2004

Abstract

We consider dynamics of chains of rigid masses connected by links described by irreversible, piecewise linear constitutive relation: the force–elongation diagram consists of two stable branches with a jump discontinuity at the transition point. The transition from one stable state to the other propagates along the chain and excites a complex system of waves. In the first part of the paper (Cherkaev et al., *Transition waves in bistable structures. I. Delocalization of damage*), the branches could be separated by a gap where the tensile force is zero, the transition wave was treated as a wave of partial damage. Here we assume that there is no zero-force gap between the branches. This allows us to obtain steady-state analytical solutions for a general piecewise linear trimeric diagram with parallel and nonparallel branches and an arbitrary jump at the transition. We derive necessary conditions for the existence of the transition waves and compute the speed of the wave. We also determine the energy of dissipation which can be significantly increased in a structure characterized by a nonlinear discontinuous constitutive relation. The considered chain model reveals some phenomena typical for waves of failure or crushing in constructions and materials under collision, waves in

*Corresponding author. Tel.: +1-801-581-7315; fax: +1-801-581-4148.
E-mail addresses: cherk@math.utah.edu (A. Cherkaev), elena@math.utah.edu (E. Cherkaev).
[1]Also for correspondence.

0022-5096/$ - see front matter © 2004 Published by Elsevier Ltd.
doi:10.1016/j.jmps.2004.08.001

a structure specially designed as a dynamic energy absorber and waves of phase transitions in artificial and natural passive and active systems.

Keywords: Dynamics; Phase transition; Bistable-bond chain; Integral transforms

1. Introduction

In Part II of the paper, we study transition waves in discrete bistable-link chains shown in Fig. 1. Typical constitutive relations are represented by piecewise linear diagrams shown in Fig. 2. Such dependencies correspond, in particular, to the waiting-link structure described in Part I if there is no zero-force gap between the branches. The transition from the first branch to the second one is assumed to be irreversible. This means that after the moment when the elongation q first time reaches the critical value q_*, the tensile force in the link of the chain is described by the second branch of the constitutive relation, and it does not return to the first branch even when the elongation decreases below q_*.

Bistable (or multi-stable) chain models were considered in many works (see Frenkel and Kontorova, 1938; Muller and Villaggio, 1977; Fedelich and Zanzotto, 1992; Rogers and Truskinovsky, 1997; Ngan and Truskinovsky, 1999, 2002; Puglisi

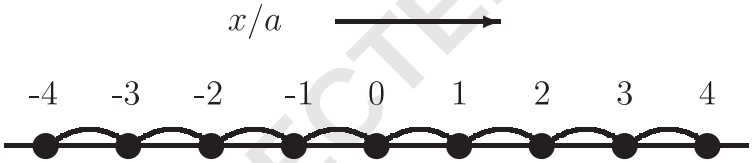

Fig. 1. The periodic chain consisting of point rigid particles of mass M connected by massless links.

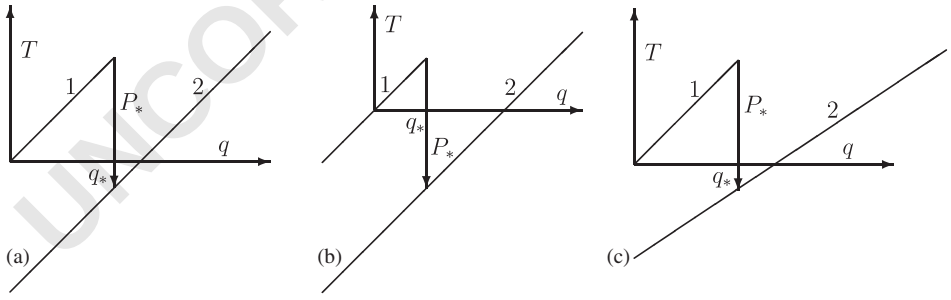

Fig. 2. The force–elongation dependence. (a) The parallel-branch piecewise linear dependence: 1. $T = \mu q$ (the first branch) and 2. $T = \mu q - P_*$ (the second branch). (b) The parallel-branch dependence for a prestressed chain that behaves as an active structure. (c) Nonparallel-branch dependence: 1. $T = \mu q$ and 2. $T = \gamma\mu q - P_{**} = \mu q - P_* - (1-\gamma)\mu(q - q_*)$.

and Truskinovsky, 2000, 2002a,b; Truskinovsky and Vainchtein (2004a,b)). First analytical solutions for waves in a free bistable chain were published by Slepyan and Troyankina (1984, 1988). Such models were also considered in Slepyan (2000, 2001, 2002) and Balk et al. (2001a,b).

The piecewise linear bistable diagram for the tensile force, T, has two linear branches: $T=\mu q$ valid before the transition, and $T=\mu q_*-P_*+\gamma\mu(q-q_*)$ valid after the moment when the elongation first reaches the critical value, $q=q_*$ (the first branch is valid for $q<q_*$ and vice versa if the transition is reversible). A particular case of two linear branches, $T=\mu q$ and $T=\gamma\mu q$ ($\gamma<1$), that is, $P_*=\mu(1-\gamma)q_*$, was examined in Slepyan and Troyankina (1984), while the case $P_*<0, \gamma>1, P_*-\mu(\gamma-1)q_*>0$ was studied in Slepyan and Troyankina (1988). A reversible diagram of such a kind with $P_*=\mu(1+\gamma)q_*$ is assumed in Kresse and Truskinovsky (submitted) for a bistable supported chain as Frenkel–Kontorova model. Reversible two-phase chains were also considered by Balk et al. (2001a,b). We now consider a free chain characterized by a general piecewise linear trimeric diagram shown in Fig. 2. with arbitrary values of $\gamma>0$ and $P_*>0$.

The dynamics of the chain is described by the equation

$$M\frac{\mathrm{d}^2u_m(t)}{\mathrm{d}t^2}=T(u_{m+1}-u_m)-T(u_m-u_{m-1}),\quad m=-\infty,\ldots,\infty, \tag{1}$$

where u_m is the displacement of the mth mass, t is time, a is the distance between two neighboring masses at rest. A nonmonotonic (and discontinuous) function T is the tensile force in the locally unstable link shown in Fig. 2, M is the mass of the particle.

We study steady-state transition waves; in this case, the velocities of the masses and the elongations of the links are functions of a single variable, $\eta=am-vt$, where m is the node number and $v=\mathrm{const}$ is the speed of the front of the transition wave. For the considered discrete chain this means that the time interval between the transition of neighboring links is equal to a/v, and $u_{k+1}(t)=u_k(t-a/v)$. In this case, the infinite system (1) can be reduced to an equivalent single equation. It is assumed here that the speed is subcritical, that is, $0<v<\min(c, c\sqrt{\gamma})$, where c is the long wave speed in the initial phase chain, $c=a\sqrt{\mu/M}$. The Fourier transform is used to integrate the obtained equation. In a general case, when the stable branches are not parallel, $\gamma\neq1$, we apply the Wiener–Hopf technique.

We derive an analytical solution for the elongations of the links and the velocities of the masses corresponding to a given (arbitrary) subcritical speed of the transition wave. This allows us to express the external force (which is assumed to be applied at infinity) as a function of the wave speed and, in particular, to find the minimal force which causes the transition. Inverting this relation we find the dependence of the speed of the transition wave on the applied force. This latter dependence is multivalued; however, only the maximal speed branch is really acceptable.

The dynamic transition in the chain is accompanied by a system of waves, waves of zero wavenumber and high-frequency oscillating waves. In the first part of the paper where the wave of transition was treated as a wave of partial damage, we showed that the high-frequency waves dissipate large amounts of energy. Here we determine the total dissipation caused by the these waves. Note that, in the

formulation of the condition at $-\infty$, we consider only the uniform part of the solution paying no attention to the oscillating waves. This looks as the latter waves freely propagate independently of the condition. In fact, we assume that, in a related real system, at least a small inelasticity exists, and the oscillating waves become negligible at a long distance.

Below we distinguish models with a parallel-branch diagram, $\gamma = 1$, and with nonparallel branches, $\gamma \neq 1$, since the corresponding mathematical problems appear different. At the same time, we show that the results for the parallel-branch case follow in a limit, $\gamma \to 1$, from those derived for the nonparallel branch case.

An outline of the wave structure. The wave systems behind and ahead of the transition wave front consist of waves satisfying the equations for homogeneous chains. The intact chain dynamics is governed by an infinite system of the equations:

$$M\frac{\mathrm{d}^2 u_m(t)}{\mathrm{d}t^2} - \mu[q_{m+1}(t) - q_m(t)] = 0, \quad q_m = u_m - u_{m-1}, \quad m = 0, \pm 1, \pm 2, \ldots, \tag{2}$$

where u_m is the displacement along the chain and μ is the stiffness of the bond. In the long-wave approximation, this equation coincides with the one-dimensional wave equation for an elastic rod

$$E\frac{\partial^2 u}{\partial x^2} - \varrho\frac{\partial^2 u}{\partial t^2} = 0, \quad E = \frac{\mu a}{S}, \quad \varrho = \frac{M}{Sa}, \tag{3}$$

where E is the elastic modulus, ϱ is the density and S is the cross-section area which does not matter in the present considerations. Note that (Eq. 2) can be rewritten in terms of the elongation as

$$M\frac{\mathrm{d}^2 q_m(t)}{\mathrm{d}t^2} + \mu[2q_m(t) - q_{m-1}(t) - q_{m+1}(t)] = 0. \tag{4}$$

Substituting into (Eq. 2) the expression for a complex wave

$$u = A\exp[\mathrm{i}(\omega t - kam)], \tag{5}$$

where A, ω, and k are an arbitrary amplitude, the frequency and the wavenumber, respectively, we obtain the dispersion relation

$$\omega = \pm 2\sqrt{\mu/M}\sin(ka/2) \tag{6}$$

as a condition for the existence of wave (5). For real k and ω phase and group velocities, v_p and v_g, of the wave are

$$v_\mathrm{p} = \frac{\omega}{k} \quad \text{and} \quad v_\mathrm{g} = \frac{\mathrm{d}\omega}{\mathrm{d}k}. \tag{7}$$

In terms of the phase velocity, the dispersion relation becomes

$$kv_\mathrm{p} = \pm 2\sqrt{\mu/M}\sin(ka/2). \tag{8}$$

For a long wave, $k \to 0$, it follows that $v_\mathrm{p} \sim \pm c$, $c = a\sqrt{\mu/M}$. For any nonzero v_p a finite number of real values of k satisfies (Eq. 8). If $v_\mathrm{p}^2 \geqslant c^2$, the only existing wave is

the one with zero wavenumber, $k=0$. For a large subcritical phase velocity, $v_p^2<c^2$, in addition to this, there exist a couple of waves with nonzero wavenumbers satisfying (Eq. 8), $k=\pm k_1$. Then, the number of waves satisfying the dispersion relation increases unboundedly with the decrease of v_p^2.

In the considered problem, in the case of a nonparallel branches of the constitutive relation, the dispersion relation for waves in the second phase chain differs only by the modulus which is equal to $\gamma\mu$ instead μ. Accordingly, the speed of a zero-wavenumber wave is $c_-=a\sqrt{\gamma\mu/M}$.

Let $v=\text{const}>0$. Three zero-wavenumber waves can exist: the first is an incident wave propagating to the right at $\eta<0$, the second is a reflective wave propagating to the left at $\eta<0$ and the third is a wave propagating to the right ahead of the transition front, i.e. at $\eta>0$. It is assumed that the elongation in the incident wave is $q=q^0=\text{const}$. Then the corresponding displacement is

$$u_m^0=q^0(m-c_-t/a)+\text{const},\quad \frac{\mathrm{d}u_m^0}{\mathrm{d}t}=-\frac{c_-}{a}q^0. \tag{9}$$

The same relation between the elongation and the particle velocity (which are also constants) is valid for such a wave at $\eta>0$, but with c instead c_-. Correspondingly, for the elongation in the reflective wave propagating to the left, $q=q_{\text{ref}}=\text{const}$, the displacement is

$$u_m^{\text{ref}}=q_{\text{ref}}(m+c_-t/a)+\text{const},\quad \frac{\mathrm{d}u_m^{\text{ref}}}{\mathrm{d}t}=\frac{c_-}{a}q_{\text{ref}}. \tag{10}$$

In contrast, the displacement in each sinusoidal wave is assumed to be a function of $\eta=am-vt$. So, the phase velocity, v, is the same for all these waves. However, the energy flux velocity in a wave is equal to its group velocity. The sinusoidal waves are caused by the transition. Hence the waves whose group velocity is below v are placed behind the front, at $\eta<0$, and vice versa.

Since the elongation and particle velocities in the waves of zero wavenumber are constants, the total values, that is, the elongation and particle velocities in sum with those for the sinusoidal waves, depend only on η as a continuous variable for any given m. This corresponds to self-similarity of the steady-state motion of the chain: the elongations, as well as the particle velocities, of different links differ from each other only by a shift in time equal to am/v. This fact allows us to consider the elongation of only one link. Recall that the steady-state dependence on η is valid for the elongations and particle velocities, but not for the total displacement because of relations (9) and (10).

For the discussed steady-state motion, (Eq. 4) becomes

$$Mv^2\frac{\mathrm{d}^2q(\eta)}{\mathrm{d}\eta^2}+\mu[2q(\eta)-q(\eta-1)-q(\eta+1)]=0. \tag{11}$$

The Fourier transform of this equation with a right-hand side, $f(\eta)$, leads to the solution as

$$q^{\mathrm{F}}(k)=\frac{f^{\mathrm{F}}(k)}{\mu[4\sin^2(ka/2)-v^2a^2k^2/c^2]}. \tag{12}$$

It can be seen that if $v_{\mathrm{p}}=v$ the denominator of this expression vanishes at those and only at those k which satisfy the dispersion relation in (Eq. 8) for $k=0$ and for $k\neq 0$. Along with this, if the load function, $f^{\mathrm{F}}(k)$, is regular, a contribution to the elongation at $\eta\to\pm\infty$ gives the integration (in the inverse transform) only in infinitesimal vicinities of the poles of $q^{\mathrm{F}}(k)$. Thus, the system of waves transferring energy to infinity really consists of waves of zero wavenumber (their phase and group velocities coincide: $v_{\mathrm{p}}=v_{\mathrm{g}}=\pm c$) and sinusoidal waves with the phase velocity equal to v. Note that there exists a discrete set of speeds where $v=v_{\mathrm{g}}$. Such a resonant case corresponds to a pole of $q^{\mathrm{F}}(k)$ of the second order. In this case, the steady-state regime does not exist in the elastic chain.

The existence of real poles of the integrand in (Eq. 12) reflects the nonuniqueness of the steady-state solution. In order to select the required particular solution a rule based on the *causality principle* is used, see Slepyan (2002). According to this principle, the steady-state solution $q(\eta)$ is considered as a limit at $t\to\infty$, of a transient solution $q(\eta,t)$ with zero initial conditions. This and some related principles are discussed in Bolotovsky and Stolyarov (1972).

In the following, we use nondimensional values taking a, c and μa as the length, speed and force units, respectively; for example,

$$u'_m=\frac{u_m}{a},\quad q'_m=\frac{q_m}{a}=u'_m-u'_{m-1},\quad v'=\frac{v}{c},\quad t'=\frac{ct}{a},$$
$$\eta'=\frac{\eta}{a}=m-v't',\quad P'_*=\frac{P_*}{\mu a} \tag{13}$$

We drop primes since this should not cause any confusion.

2. Waves of transition: parallel branches

2.1. Formulation

An equivalent problem. Consider an infinite irreversible bistable chain shown in Fig. 1, with parallel branches of the force–elongation dependence shown in Fig. 2(a). The transition to the second branch of the diagram generates a drop of the tensile force at the moment $t=t_*$ when the elongation q first time reaches the critical value, $q=q_*$. This nonlinear dependence can be modelled using an *equivalent* problem which considers the intact linear chain with the bonds corresponding to the first branch of the diagram. At the moment $t=t_*$ in the *equivalent* problem a pair of external forces $\mp P_*$ is instantly applied to the left and right masses connected by this bond, respectively, as it is shown in Fig. 3(a).

The motion of chain masses in the *equivalent* problem is the same as in the *original* problem. Indeed, the applied pair of forces together with the tensile force in the first-branch bond acts on the masses as the tensile force in the second branch of the

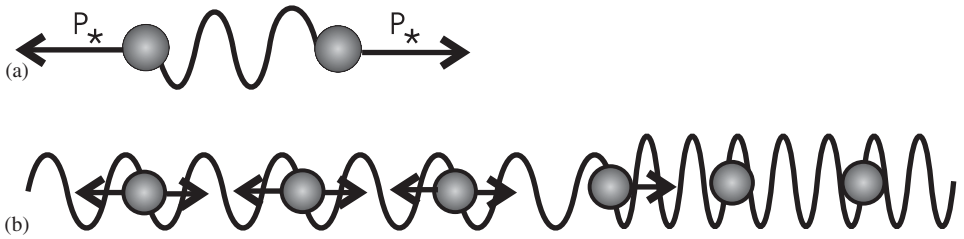

Fig. 3. The difference P_* between the forces in the *original* and *equivalent* problems is compensated by a couple of external forces: (a) The forces for a bond. (b) The forces behind the transition front mutually annihilate each other.

force–elongation dependence in the *original* problem. Hence, the particle displacements and the strain of bonds are the same for the *original* and the *equivalent* problems. At the same time, the tensile forces in the second-branch bonds in the *original* problem differ by $-P_*$ from that of the corresponding first-branch bonds in the *equivalent* problem. Thus, the parallel-branch problem can be considered as a linear one, and only these additional external forces in the *equivalent* problem reflect the nonlinearity.

Note that if all the bonds to the left of some mass correspond to the second branch, while all the bonds to the right correspond to the first branch, the resulting external force must be applied to this mass only. The other external forces mutually annihilate each other as this can be seen in Fig. 3(b). Below we consider the *equivalent* problem taking into account the difference in the tensile force.

The nondimensional equation for the bistable, parallel branch chain follows from (Eq. 2) with the linear dependence

$$q_m(t) = u_m(t) - u_{m-1}(t) \tag{14}$$

and the external forces on the right-hand side:

$$\frac{\mathrm{d}^2 u_m(t)}{\mathrm{d}t^2} - q_{m+1}(t) + q_m(t) = \begin{cases} 0 & \text{if } (1,1), \\ -\hat{P}_* & \text{if } (1,2), \\ \hat{P}_* & \text{if } (2,1), \\ 0 & \text{if } (2,2), \end{cases} \tag{15}$$

where the pairs $(1,1),\ldots,(2,2)$ denote the state (the first branch (1) or the second one (2)) of the bonds connecting the mth mass with the left and the right neighbors, respectively.

Remark 1. When the chain is initially uniformly prestressed, the linearity of the problem allows us to consider additional dynamic field using the same equations with the force–elongation dependence presented in Fig. 2(b).

Steady-state formulation. Assume that the transition wave propagates to the right with a constant speed, $v>0$. Then, the nondimensional time interval between the

transition of neighboring bonds is equal to $1/v$. In this case, we can consider the steady-state regime with

$$\frac{\mathrm{d}q_m(t)}{\mathrm{d}t} = -v\frac{\mathrm{d}q(\eta)}{\mathrm{d}\eta} \quad (\eta = m - vt). \tag{16}$$

From (Eq. 15) it follows that [compare with the dynamic equation (4)]

$$v^2\frac{\mathrm{d}^2q(\eta)}{\mathrm{d}\eta^2} + 2q(\eta) - q(\eta-1) - q(\eta+1) = P_*[2H(-\eta) - H(-\eta-1) - H(-\eta+1)]. \tag{17}$$

The speed of the transition wave is a function of the amplitude of the incident wave. However, it is more convenient to consider the problem for a given speed and to determine the incident wave as a function of the speed. Since the speed is an explicit parameter of the problem, this approach leads to a direct problem instead of the inverse one. Moreover, we will show below that the dependence on the speed is a single-valued function, while the inverse dependence is not.

To determine such a dependence we need an additional condition; it is the transition condition

$$q(0) = q_*. \tag{18}$$

Recall that the transition front coordinate corresponds to $\eta = 0$.

A subcritical transition wave speed is assumed, that is, the nondimensional transition front speed satisfies the inequalities

$$0 < v < \min(\gamma, 1). \tag{19}$$

Conditions at infinity. To complete the formulation we have to introduce conditions at infinity. We start with a semi-infinite chain, $m = -N, -N+1, \ldots$, assuming number N to be large enough (later, this number will be assigned $-\infty$). We consider two types of excitation conditions which lead to the same solution.

(1) Assume that a constant, directed to the left tension force $\mathscr{P}$ is applied to the end mass, $m = -N$, at the time instant $t = -N/v$.

(2) Alternatively, this mass is forced to move with a constant speed, $\mathrm{d}u_{-N}/\mathrm{d}t = -w$.

The transition from the first branch of the diagram to the second one in the first bond (in the bond connecting the particle $m = -N$ with the chain) corresponds to applying external forces $\mp P_*$ in the *equivalent* problem. These forces are applied to the particles $m = -N$ and $m = -N+1$. When the transition wave reaches the next bond, the force at the particle with the number $m = -N+1$ is cancelled, but it arises at the particle numbered $m = -N+2$, and so on. In this process, two forces act all the time: one equal to $-P_*$ is applied to the end particle, $m = -N$, while the other equal to P_* is applied to the particle at the transition wave front. The same considerations are valid for the case where a constant speed at the end mass is assumed.

For the condition at the right, $m \to \infty$, we assume that there is no energy flux *from* infinity. So, ahead of the transition front, for $m \to \infty$ only those waves can exists whose group velocities exceed the transition front velocity v.

2.2. Solution

Because of linearity of the *equivalent* problem, the strain $q(\eta)$ can be represented as a sum of a homogeneous solution q^0 of (Eq. 17) (that corresponds to a zero wavenumber incident wave caused by an external action at $\eta = -\infty$) and an inhomogeneous solution $q(\eta)$ (that corresponds to waves excited by the right-hand side forces). The incident wave moves to the right with the unit nondimensional speed larger than the speed of the transition front. In the considered case, in (Eq. 9) $c_- = c$, and in terms of the nondimensional variables this wave is characterized by

$$q = q^0, \quad \frac{\mathrm{d}u}{\mathrm{d}t} = -q^0. \tag{20}$$

To distinguish the solution of the inhomogeneous equation (17) we denote the corresponding elongations by $q(\eta)$. Using the Fourier transform

$$q^{\mathrm{F}}(k) = \int_{-\infty}^{\infty} q(\eta) \exp(\mathrm{i}k\eta)\, \mathrm{d}\eta \tag{21}$$

on η as a continuous variable (or, equivalently, the Fourier transform on $-vt$ for $m = 0$) we obtain

$$q^{\mathrm{F}}(k) = \frac{2P_*(1-\cos k)}{\mathrm{i}kh(k)},$$
$$h(k) = (0 + \mathrm{i}kv)^2 + 2(1 - \cos k), \tag{22}$$

where, in accordance with the rule based on the causality principle for a steady-state solution (see Slepyan, 2002), we write $0 + \mathrm{i}kv$ instead $\mathrm{i}kv$,

$$0 + \mathrm{i}kv = \lim_{s \to +0} (s + \mathrm{i}kv). \tag{23}$$

When $s = +0$ the function $h(k)$ has a double zero at $k = 0$ and a number of real zeros at $k \neq 0 : \pm h_1, \pm h_2, \ldots, \pm h_{2n+1}$. The number of zeros increases when v decreases, see Fig. 4. These zeros reflect propagating waves which can exist in the chain. In addition, there is an infinite set of complex zeros located outside the real axis symmetrically with respect to the real and imaginary axes. They correspond to exponentially decreasing waves which do not transport energy.

Remark 2. The complex zeros, in contrast to the real ones, do not create difficulties in the computation of the integral as the inverse Fourier transform over the real axis

$$q(\eta) = \frac{1}{2\pi} \int_{-\infty}^{\infty} q^{\mathrm{F}}(k) \exp(-\mathrm{i}k\eta)\, \mathrm{d}k. \tag{24}$$

Note that this integral can be represented by a set of residues (we will use this approach below for the determination of the asymptotes for $\eta \to \pm\infty$). Here,

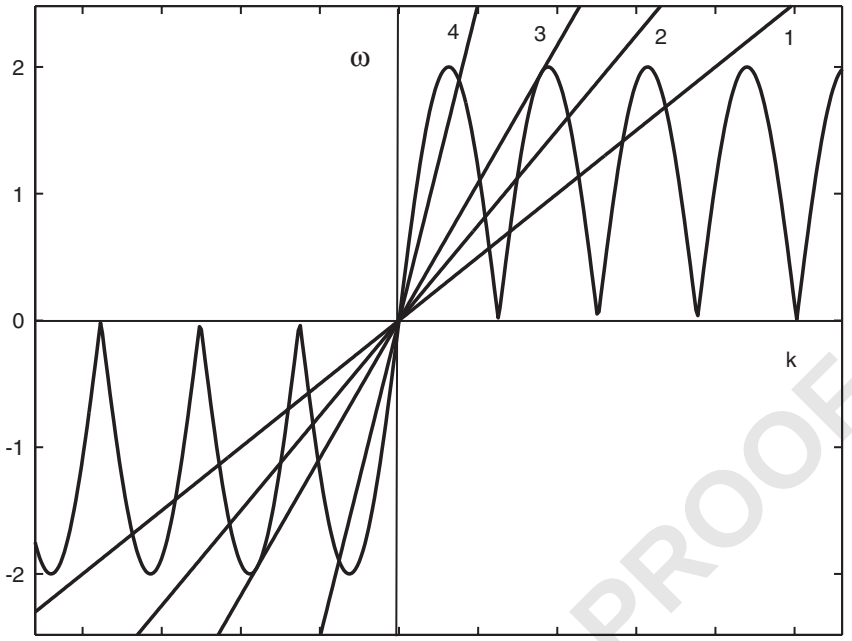

Fig. 4. The zeros, h_v, of $h(k)$ defined by the equation $\omega(k) = 2|\sin k/2|\,\mathrm{sign}\,x = kv$: 1. Five positive zeros for $v = 0.1$; 2. Three positive zeros for $v = 0.15$; 3. For $v = v_0 = -\cos k_0/2 \approx 0.217233628$ ($k = k_0 \approx 8.986818915$ is the first positive root of equation $\tan k/2 = k/2$) two of three zeros coincide (this is a resonant speed); 4. Single positive root for $v = 0.5$. As can be seen the group velocity, $\mathrm{d}\omega(h_v)/\mathrm{d}k$ at $k = \pm h_v$ exceeds the phase velocity, $\omega(k)/k$, for even v and is below the latter for odd v (for the resonant case, $v = v_0$, the group and phase velocities are the same). This implies that sinusoidal waves (h_v are their wavenumbers) excited by the transition front, propagating with the speed v, are placed ahead of the front for even v and behind the front for odd v. The steady-state regime does not exist at the resonant speed, see Fig. 5.

however, we explicitly compute the integral; therefore, the explicit expressions for the complex zeros are of no interest.

For real values of k the function $h(k)$ can be represented as

$$h(k) = h_+(k, kv)h_-(k, kv), \quad h_\pm = \omega(k) \mp kv, \quad \omega(k) = 2|\sin(k/2)|\mathrm{sgn}k. \tag{25}$$

The dispersion relations, $h_+ = 0$ and $h_- = 0$, correspond to free waves with the phase velocities $\pm v$. The corresponding real zeros $k = h_v > 0, v = 1, 2, \ldots, 2n + 1$ ($n = 0, 1, \ldots$), are the wavenumbers of these waves; symmetrical zeros, $k = -h_v$, also exist. We need to consider only the positive phase velocity mode, i.e. the equation $h_+ = 0$.

Perturbation of the real roots. In the limit when $s = +0$, the integrant of (Eq. 24) contains a number of real poles of $q^{\mathrm{F}}(k)$. So, this inversion integral, as it is, has no sense. However, we need to compute the limit of the integral, not the integral of the limit. To this end we consider here the prelimiting expression, $s + \mathrm{i}kv$ with $s \to +0$

instead $0 + \mathrm{i}kv$ (in the latter expression the symbol '0' only indicates the structure of the prelimiting expression). For the considered mode the location of the perturbed poles can be found as the asymptotic solution of the perturbed equation

$$h_+(k, kv - \mathrm{i}s) = 0 \quad (s \to +0). \tag{26}$$

We denote the roots of this equation $k = \pm h_v + \delta$, where δ is the perturbation of the root; $\delta \to 0$ if $s \to +0$. (Eq. 26) can now be rewritten as

$$[v_{\mathrm{g}}(h_v) - v]\delta \sim -\mathrm{i}s, \tag{27}$$

where

$$v_{\mathrm{g}}(k) = \frac{\mathrm{d}\omega(k)}{\mathrm{d}k} \tag{28}$$

is the group velocity, and it is assumed that $v_{\mathrm{g}} \neq v$. Thus, in the limit $s = +0$, the perturbed roots are

$$\begin{aligned} &k = \pm h_v + \mathrm{i}0 \quad [v_{\mathrm{g}}(h_v) < v], \\ &k = \pm h_v - \mathrm{i}0 \quad [v_{\mathrm{g}}(h_v) > v]. \end{aligned} \tag{29}$$

As it seen in Fig. 4, the first inequality is valid for odd v, while the second inequality is valid for even v. Hence,

$$k = \pm h_{2v+1} + \mathrm{i}0, \quad k = \pm h_{2v} - \mathrm{i}0. \tag{30}$$

Note that this separation of the poles results in the proper disposition of the sinusoidal waves as it was discussed in the Introduction.

The double root of $h(k)$ at zero is split into two. From the equation

$$2(1 - \cos k) - (kv - \mathrm{i}s)^2 = 0 \tag{31}$$

with $k \to 0$ and $s \to 0$ we find these two roots

$$k = k_1 \sim \frac{\mathrm{i}s}{1 + v}, \quad k = k_2 \sim -\frac{\mathrm{i}s}{1 - v}. \tag{32}$$

Perturbed path of the inverse Fourier transform. The inverse Fourier transform (24) corresponding to transform (22) is now completely defined. The perturbed singularities move to the upper or lower half-planes and the path of integration goes below or above of them. To calculate the limit of the integral for $s \to +0$, infinitesimal segments of the integration path below a pole at $k = h_{2v+1} + \mathrm{i}0$ or above the pole at $k = h_{2v} - \mathrm{i}0$ can be deformed downward or upward, respectively, to a half-circle with the center at the pole. The same can be made for each simple perturbed pole at $k = +\mathrm{i}0$ and at $k = -\mathrm{i}0$. As a result, the integral $q(\eta)$ can be represented as a sum of half-residues at the poles and the Cauchy principal value of the remaining part of integral (24).

Note that a half-residue at a pole of the type

$$q^{\mathrm{F}}(k) \sim \frac{A_v}{k - h_v \mp \mathrm{i}0}, \quad A_v = \mathrm{const}, \tag{33}$$

is

$$\int_{\gamma_-} \frac{A_{2v+1}}{k-h_{2v+1}-\mathrm{i}0}\exp(-\mathrm{i}k\eta)\,\mathrm{d}k = A_{2v+1}\pi\mathrm{i}\,\exp(-\mathrm{i}h_{2v+1}\eta),$$

$$\int_{\gamma_+} \frac{A_{2v}}{k-h_{2v}+\mathrm{i}0}\exp(-\mathrm{i}k\eta)\,\mathrm{d}k = -A_{2v}\pi\mathrm{i}\,\exp(-\mathrm{i}h_{2v}\eta), \tag{34}$$

where $\gamma_{\mp}$ are the lower and the upper half-circle, respectively.

In the vicinities of the real poles, the function $q^{\mathrm{F}}(k)$ has the following representation:

$$q^{\mathrm{F}}(k) \sim -\frac{\mathrm{i}P_*k}{1-v^2}\left(k-\frac{\mathrm{i}s}{1+v}\right)^{-1}\left(k+\frac{\mathrm{i}s}{1-v}\right)^{-1}$$

$$= \frac{P_*}{2}\left[\frac{1}{s+\mathrm{i}(1+v)k}-\frac{1}{s-\mathrm{i}(1-v)k}\right] \quad (s\to+0,\ k\to 0),$$

$$q^{\mathrm{F}}(k) \sim -\frac{\mathrm{i}P_*v^2h_v}{(k-h_v+\mathrm{i}\varepsilon)\,\mathrm{d}h(h_v)/\mathrm{d}k} \quad (s\to+0,\ k\to h_v),$$

$$q^{\mathrm{F}}(k) \sim -\frac{\mathrm{i}P_*v^2h_v}{(k+h_v+\mathrm{i}\varepsilon)\,\mathrm{d}h(h_v)/\mathrm{d}k} \quad (s\to+0,\ k\to -h_v), \tag{35}$$

where $k=h_v, v=1,2,\ldots,2n+1,\ n=0,1,\ldots,$ are the positive zeros of $h(k)$; the same asymptotes correspond to the negative zeros, $k=-h_v$. The sign of ε is either positive or negative, $\varepsilon=-s$ for odd v and $\varepsilon=s$ for even v, and it is assumed that $\mathrm{d}h/\mathrm{d}k\neq 0$ at these zeros of $h(k)$.

Inverse Fourier transform. We now obtain

$$q(\eta) = -\frac{P_*v}{2(1-v^2)} + P_*\sum_{v=0}^{n}\left[Q_{2v+1}\cos(h_{2v+1}\eta) - Q_{2v}\cos(h_{2v}\eta)\right]$$

$$-\frac{2P_*}{\pi}V.p.\int_0^\infty \frac{1-\cos k}{k[2(1-\cos k)-k^2v^2]}\sin(k\eta)\,\mathrm{d}k, \tag{36}$$

where

$$Q_{2v+1} = \frac{v^2h_{2v+1}}{2(\sin h_{2v+1} - v^2h_{2v+1})},$$

$$Q_{2v} = \frac{v^2h_{2v}}{2(\sin h_{2v} - v^2h_{2v})}, \quad Q_0 = 0. \tag{37}$$

Note that the principal-value integral in (Eq. 36) does not depend on the indication of the limit ($s\to 0$), and we write $-k^2v^2$ instead $(0+\mathrm{i}kv)^2$.

Thus, the transition wave is presented as a sum of the sinusoidal waves with the wavenumbers h_v and amplitudes Q_v plus a constant plus a remaining integral term. The magnitude of all terms is proportional to the excitation P_*, that is to the elongation caused by the transition.

The number n of the waves depends on the speed v. For instance, only a single cosine wave propagates ($n=1$) if $1>v>v_0=-\cos(k_0/2)\approx 0.217233628$. In this

case, $k = k_0 \approx 8.986818915$ because k_0 is the first positive root of Eq. (22) or, equivalently, $\tan k/2 = k/2$.

Strain at the transition front and distant asymptotes. Note that the strain is continuous at $\eta = 0$. The inhomogeneous, Eq. (36), and the homogeneous, q^0, parts of the solution give us in sum the expression for the total strain at $\eta = 0$ as

$$q_{\text{total}}(0) = q^0 - \frac{P_* v}{2(1-v^2)} + P_* \sum_{v=0}^{n} (Q_{2v+1} - Q_{2v}). \tag{38}$$

From Eqs. (18), where $q(0)$ means the total elongation, and from Eq. (38) we find that

$$q^0 = q_* + \frac{P_* v}{2(1-v^2)} - P_* \sum_{v=0}^{n} (Q_{2v+1} - Q_{2v}). \tag{39}$$

To find asymptotes for $\eta \to \pm\infty$ we choose another way of the calculation of the inverse-transform integral. Deform the integration path from the real axis upward for $\eta<0$ and downward for $\eta>0$ (to have the exponential multiplier vanished when $k \to \pm i\infty$) without crossing the poles. In this way, the result is expressed as an infinite set of the residues (but not the half-residues!); however, contributions of the poles with nonzero imaginary parts vanish at $\eta \to \mp\infty$, and only a finite number of contributions from the real poles remains. Referring to Eqs. (35) and (39) we get the following.

The reflective uniform wave is

$$q_{\text{ref}} = \frac{P_*}{2(1+v)} \quad (\eta<0). \tag{40}$$

The uniform wave propagating ahead of the transition front is

$$q_{\text{head}} = -\frac{P_*}{2(1-v)} + q^0 = q_* - \frac{P_*}{2(1-v^2)} - P_* \sum_{v=0}^{n} (Q_{2v+1} - Q_{2v}) \quad (\eta>0). \tag{41}$$

Asymptotes for the total elongations are

$$\begin{aligned} q_{\text{total}}(\eta) &\sim q_* + \frac{P_*}{2(1-v^2)} - P_* \sum_{v=0}^{n} (Q_{2v+1} - Q_{2v}) \\ &\quad + 2P_* \sum_{v=0}^{n} Q_{2v+1} \cos(h_{2v+1}\eta) \quad (\eta \to -\infty), \\ q_{\text{total}}(\eta) &\sim q_* - \frac{P_*}{2(1-v^2)} - P_* \sum_{v=0}^{n} (Q_{2v+1} - Q_{2v}) \\ &\quad - 2P_* \sum_{v=0}^{n} Q_{2v} \cos(h_{2v}\eta) \quad (\eta \to \infty). \end{aligned} \tag{42}$$

Tensile force and particle velocity in the uniform waves. Further we find expressions for the tensile force and the particle velocity corresponding to the uniform (zero wavenumber) waves behind the transition front. It follows from Eqs. (39) and (40)

that the constant part of the tensile force in the second branch of the dependence for the *original* problem is

$$T = q^0 + q_{\rm ref} - P_* = q_* - \frac{1-2v^2}{2(1-v^2)}P_* - P_*\sum_{v=0}^{n}\left(Q_{2v+1} - Q_{2v}\right) \quad (\eta<0). \tag{43}$$

Computing the particle velocity we recall that there are two uniform waves behind the transition front: one is the incident wave (with the strain q^0) propagating to the right, and the other is the reflected wave caused by the transition; it propagates to the left with the unit nondimensional speed. The nondimensional particle velocities in the former and the latter are [see Eq. (20)]

$$\frac{{\rm d}u}{{\rm d}t} = -q^0 \quad \text{and} \quad \frac{{\rm d}u}{{\rm d}t} = q_{\rm ref} \quad (\eta<0), \tag{44}$$

respectively. The total uniform particle velocity is thus

$$\frac{{\rm d}u}{{\rm d}t} = \frac{P_*}{2(1+v)} - q^0 = -q_* + \frac{1-2v}{2(1-v^2)}P_* + P_*\sum_{v=0}^{n}\left(Q_{2v+1} - Q_{2v}\right) \quad (\eta<0). \tag{45}$$

The nondimensional tensile force and particle velocities ahead of the transition front are equal to the strain q and $-q$, respectively. Recall that the particle velocities are the same for the *original* and *equivalent* problems.

Calculation of the speed v. The obtained solution depends on the speed v which is still unknown. It can be determined using the condition at $\eta \to -\infty$ ($m = -N$) as the applied force $\mathscr{P}$ equal to the uniform part of the tensile force T, or as a given uniform part of the particle velocity $-w$. The corresponding relations follow from Eqs. (43) and (45) as

$$\begin{aligned} &\frac{1-2v^2}{2(1-v^2)}P_* + P_*\sum_{v=0}^{n}\left(Q_{2v+1} - Q_{2v}\right) = q_* - \mathscr{P}, \\ &\frac{1-2v}{2(1-v^2)}P_* + P_*\sum_{v=0}^{n}\left(Q_{2v+1} - Q_{2v}\right) = q_* - w. \end{aligned} \tag{46}$$

It can be seen now that the solution depends only on the ratios

$$\mathscr{P}^0 = \frac{\mathscr{P}}{q_*}, \quad P_*^0 = \frac{P_*}{q_*}, \quad w^0 = \frac{w}{q_*}, \tag{47}$$

but not on the parameters $\mathscr{P}, P_*$ and w themselves.[2] In these terms, the above equations become

[2]These ratios could be used of course as nondimensional values from the very beginning; however, we introduce them only now to avoid a nonusual form of some relation for the waves.

$$\frac{1-2v^2}{2(1-v^2)}P_*^0 + P_*^0\sum_{v=0}^{n}(Q_{2v+1}^0 - Q_{2v}^0) = 1-\mathscr{P}^0,$$

$$\frac{1-2v}{2(1-v^2)}P_*^0 + P_*^0\sum_{v=0}^{n}(Q_{2v+1}^0 - Q_{2v}^0) = 1-w^0. \tag{48}$$

Eqs. (48) serve for the determination of the transition wave speed v. They contain two nondimensional parameters; parameter P_*^0 defines the material properties, and $\mathscr{P}^0$ or w^0 describes the level of external excitation.

2.3. Discussion of the results

Dependencies (48) are shown in Fig. 5. We notice peaks in the dependence on the speed v. These peaks (they are infinite) correspond to the resonant values of the transition wave speed which cannot be achieved in the steady-state regime. For the resonant speed, the group and phase velocities coincide, that is, the ray $\omega = kv$ is tangent to the dispersion curve $\omega(k) = 2|\sin k/2|\text{sign}\, k$, see case 3 in Fig. 4. When the phase velocity, i.e. the transition wave speed increases and approaches the resonant level, the two waves (with the wavenumbers tending to each other) coincide, see Fig.

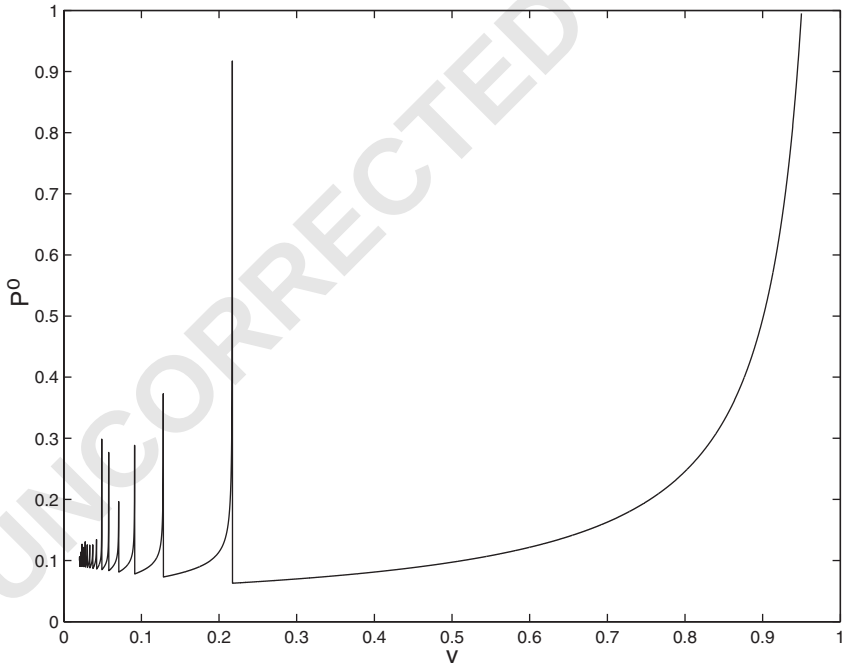

Fig. 5. The external action level versus the transition front speed: Nondimensional tension force $\mathscr{P}^0$ as a function of the speed, v. The (infinite) peaks correspond to the resonant speeds where two zeros of $h(k)$ coincide, see Fig. 4.

4. In this way, the amplitudes of the waves increase unboundedly, and this is reflected by the lifted graphs in Fig. 5. After the speed exceeds the resonance level the graph immediately drops to a 'regular' level because the mentioned two waves are not excited at the post-critical regime.

Note, that such infinite peaks exist only in the steady-state solution; they reflect the discontinuity in the assumed constant-speed solution that depends on v as a parameter. There are no discontinuities in a time-dependent solution with an increasing speed crossing the resonant level. In this transient case, the peak is finite and it's height depends on how fast the resonant level is passed. Therefore, the peaks are not insurmountable obstacles as they look in Fig. 5, and the wave speeds above the main resonance speed are not forbidden.

In fact, only the waves with these high speeds are realizable. Indeed, considering whether or not the transition occurs at $\eta = 0$ we have to check if the elongation at $\eta > 0$ is below the critical level. This is the case in the high-speed region where the resistance monotonically grows with the speed. This phenomenon for the crack propagation in a discrete lattice was noted and investigated by Marder and Gross (1995). Numerical results discussed below help to elucidate this point.

2.4. Energy relations

From Eqs. (43) and (45) it follows that in terms of the nondimensional values

$$w^0 = \mathscr{P}^0 + \frac{v}{1+v} P^0_*. \tag{49}$$

The energy flux from $\eta = -\infty$ caused by the external force $\mathscr{P}^0$ is

$$N^0 = \mathscr{P}^0 w^0 = \mathscr{P}^0 \left(\mathscr{P}^0 + \frac{v}{1+v} P^0_* \right) = w^0 \left(w^0 - \frac{v}{1+v} P^0_* \right). \tag{50}$$

This energy flux increases the strain and kinetic energies of the chain. A part of this energy corresponds to the 'macrolevel' chain dynamics, that is to the waves which are uniform in each region, $\eta < 0$ and $\eta > 0$. The other part is carried away from the transition front by the sinusoidal waves, see Eq. (36). This latter part can be considered as the dissipation (as a *wave dissipation*). The wave dissipation can be calculated as the difference between the energy flux (50) and the macrolevel energy flux in the uniform wave ahead of the transition front [the latter is equal to $-q_{\text{head}}\, \mathrm{d}u/\mathrm{d}t$ at $\eta > 0$, see Eq. (41)].

There is a more straightforward way to calculate the dissipation per unit time. Consider the macrolevel energy release rate per unit length G^0 equal to the difference between the work produced during the transition and the energy required for the transition, see Fig. 6. Both ways lead to the same result:

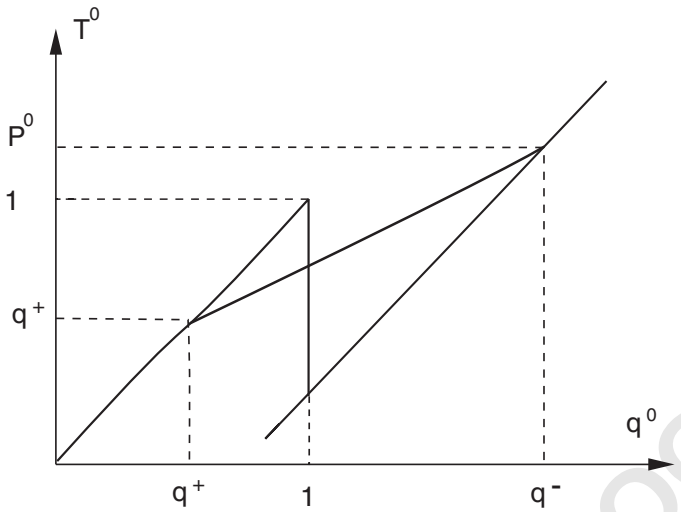

Fig. 6. The nondimensional energy dissipation as the difference between the transition work and the increase of the strain energy during the transition on the macrolevel. The former is defined by the trapezium $(q^+,0)$, (q^+,q^+), $(q^-,\mathscr{P}^0)$, $(q^-,0)$, while the latter is numerically equal to the area under the dependence within the segment q^+,q^-.

$$
\begin{aligned}
&D^0 = G^0 v = (\mathscr{G} - U)v,\\
&\mathscr{G} = \frac{1}{2}(\mathscr{P}^0 + q^+)(q^- - q^+),\\
&U = \frac{1}{2}(q^-)^2 - \frac{1}{2}(q^+)^2 - P^0_*(q^- - 1),\\
&q^+ = \mathscr{P}^0 - \frac{v^2}{1-v^2}P^0_*,\\
&q^- = \mathscr{P}^0 + P^0_*.
\end{aligned}
\tag{51}
$$

Here the nondimensional values are used in accordance with Eq. (47); $\mathscr{G}$ is the transition work per unit length, U is the strain energy increase due to the transition, $q^{\pm}$ are the uniform parts of the nondimensional strain, divided by q_*, for $\eta>0$ and $\eta<0$, respectively[see Eqs. (39)–(41)].

From system Eqs. (51) we compute

$$D^0 = \left[\frac{1-2v^2}{2(1-v^2)}P^0_* + \mathscr{P}^0 - 1\right]P^0_* v. \tag{52}$$

In terms of dimensional variables, the wave dissipation can be rewritten as

$$\hat{D} = \left[\frac{1-2v^2/c^2}{2(1-v^2/c^2)}P_* + \mathscr{P}_0 - \mu q_*\right]\frac{P_* v}{\mu a}. \tag{53}$$

The Maxwell dissipation-free transition would correspond to zero wave

dissipation or to the relation

$$\frac{1-2v^2}{2(1-v^2)}P_*^0+\mathscr{P}^0-1=0. \tag{54}$$

In this hypothetic case, the transition line on the dependence crosses the jump vertical segment at the middle as shown in Fig. 6. Because of the wave dissipation, the transition occurs at larger values.

The dissipation – energy flux ratio

$$\lambda=\frac{D}{N}=vP_*^0\left[\frac{1-2v^2}{2(1-v^2)}P_*^0+\mathscr{P}^0-1\right]\left[\mathscr{P}^0\left(\mathscr{P}^0+\frac{v}{1+v}P_*^0\right)\right]^{-1} \tag{55}$$

as a function of P_*^0 for some values of $\mathscr{P}^0$ is presented in Fig. 7.

Note that the parallel-branch diagram for a bistable chain with a nonlocal interaction (the chain particles interact with four neighbors, but only the nearest-neighbor interaction is bistable) is briefly considered in Truskinovsky and Vainchtein (2004b). In particular, the dissipation for the case $P_*^0=1$ is found.

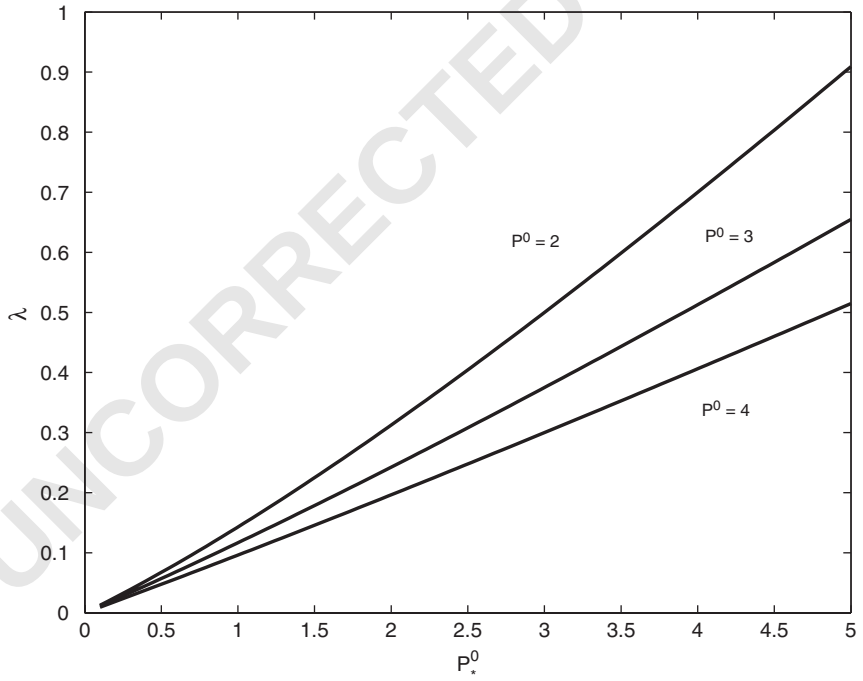

Fig. 7. The energy dissipation ratio λ for the wave speed $v=0.5$ as a function of the jump P_*^0 for different $\mathscr{P}^0$.

2.5. Transient regimes

A finite chain consisting of 32 cells was examined numerically. Point $m = 0$ was fixed, while the end particle, $m = 32$, was the subject of an impact. The results presented in Fig. 8 correspond to the dynamics of the initially unstressed resting chain with $P_*^0 = 1$. For $t > 0$ the chain is under a given constant velocity of the end particle. In particular, this case was examined to compare the speeds of the transition front derived analytically from Eq. (48) and computed numerically. A good agreement between the analytical and numerical results was found. This is also shown in Fig. 9 where the numerical results are marked by asterisks. Dynamic behavior of the chain under an inelastic impact of the end particle by a rigid mass is

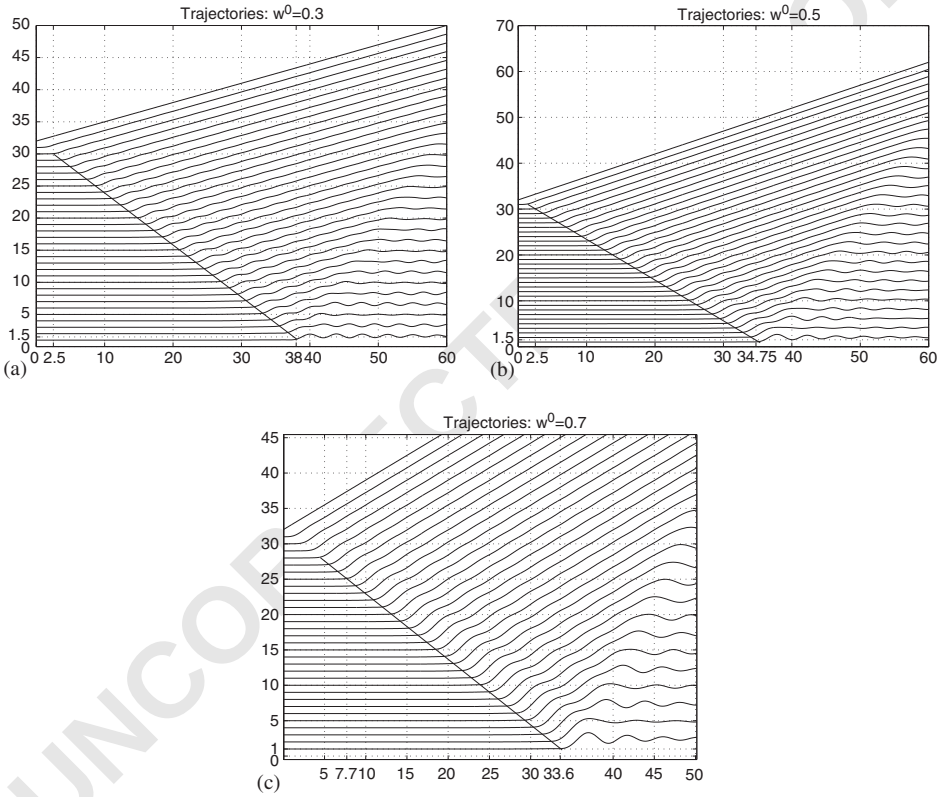

Fig. 8. Position of the knots versus time for a 32-cell chain under a given velocity, w^0, of the end particle: (a) $w^0 = 0.3$, (b) $w^0 = 0.5$, (c) $w^0 = 0.7$. The chain with the jump discontinuity of the dependence $P_*^0 = 1$ is initially unstressed and unmoving. For $t > 0$ the chain is under a given constant velocity of the end particle. A weak elastic wave propagates with the unit (nondimensional) speed; the transition front is marked by an inclined straight line, its speed numerically evaluated from the graph is shown by asterisks in Fig. 9 in comparison with the results of analytical calculation using Eq. (23). The elastic wave reflection off the fixed point seen in the graphs can cause an opposite transition wave.

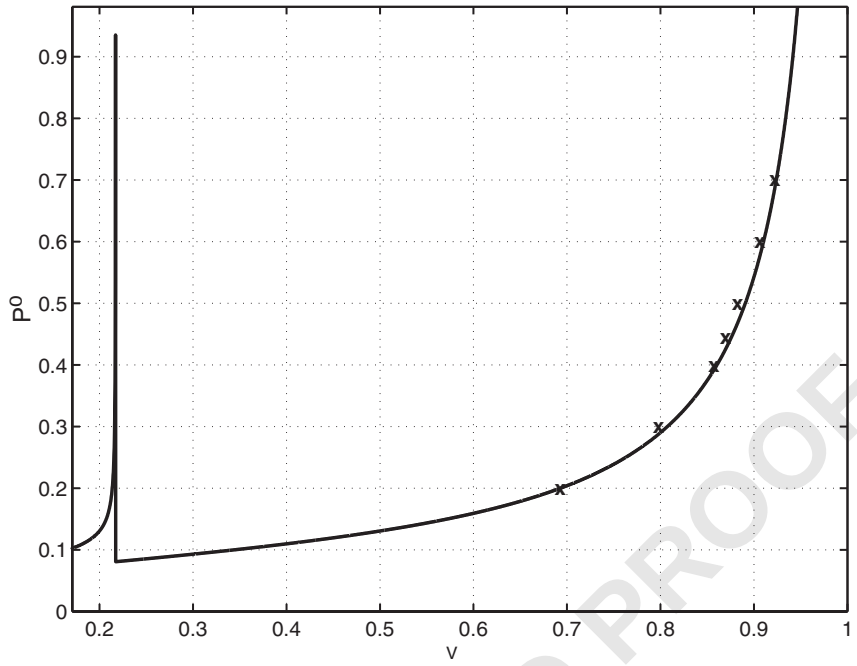

Fig. 9. Speed of the transition front analytically calculated using Eq. (23). Numerically evaluated transition wave speed is shown by asterisks.

presented in Fig. 10. This case corresponds to the conditions of an initial speed $w^0 = \mathrm{d}u_{32}(0)/\mathrm{d}t$ of an increased end mass $M^0 \geqslant 1$.

3. Waves of transition: nonparallel branches

3.1. Formulation and solution

We now consider a general case of the constitutive relation assuming that the branches of the force–elongation diagram also differ by the modules:

$$T = \begin{cases} q & \text{if } t < t_*, \\ \gamma q - P_{**} & \text{if } t > t_*. \end{cases} \tag{56}$$

We use here the nondimensional values; t_* is the instance of the transition. The distance from the first branch to the other at $q = 0$, P_{**}, is expressed through the jump, P_*, and the critical elongation, q_*, as (see Fig. 2(c))

$$P_{**} = P_* - (1 - \gamma)q_*. \tag{57}$$

The parallel-branch case considered above corresponds to $\gamma = 1$.

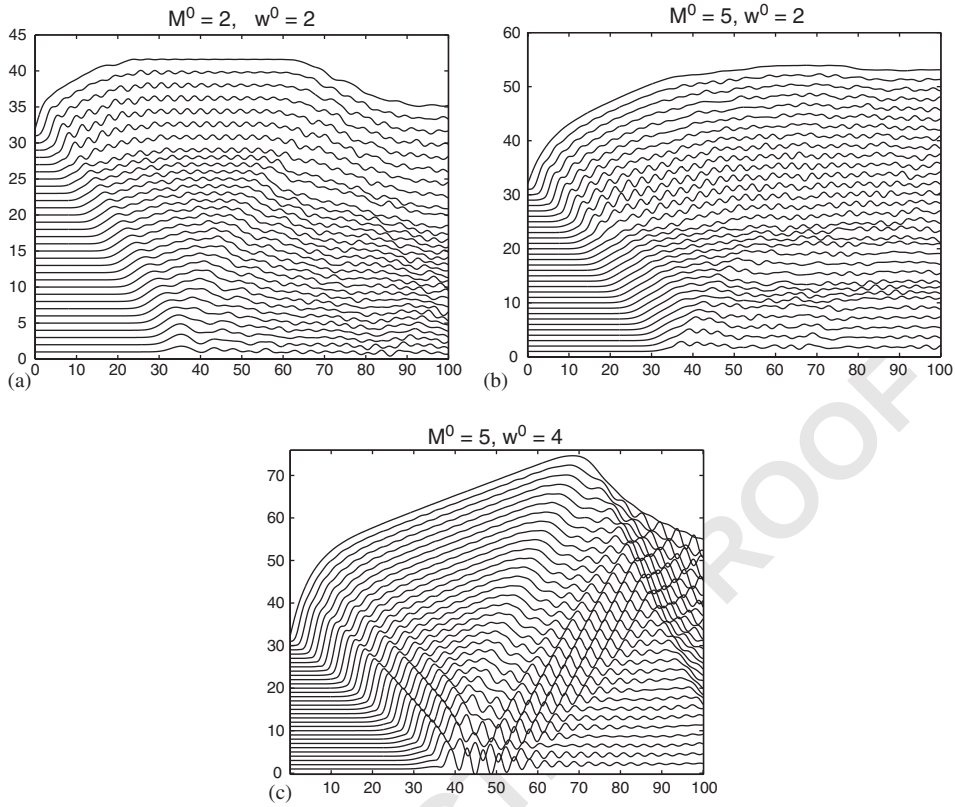

Fig. 10. Position of the knots versus time for a chain with the dependence shown in Fig. 2(a) under an impact of the end particle ($P_*^0 = 1$): (a) A weak impact, $M^0 = 2, w^0 = 2$. The transition wave propagates only over a part of the chain. (b) A moderate impact, $M^0 = 5, w^0 = 2$. An opposite transition wave arises under the reflection of the elastic wave off the fixed point. (c) A strong impact, $M^0 = 5, w^0 = 4$. The transition envelopes the whole chain.

Equivalent problem. We begin with a formulation similar to that for the parallel-branch dependence, namely, we consider an intact chain under the external forces which compensate the difference between the branches. In the considered case, however, these additional forces depend on the elongation. This compensation changes the left-hand side of the dynamic equation in the region where the forces are applied. So, we face a mixed problem with different equations (or the same equation, but with different parameters) in different regions.

For the *equivalent* problem, in terms of the nondimensional variables as in Eq. (13), the condition at $-\infty$ becomes

$$T^- = \mathscr{P} + P_* + (1-\gamma)(q_u - q_*), \tag{58}$$

or, since in this problem $T^- = q^-$

$$q^- = \frac{1}{\gamma}[\mathscr{P} + P_* - (1-\gamma)q_*] \quad (\eta = -\infty), \tag{59}$$

where the superscript '−' is used to indicate the uniform parts of the values at $\eta<0$. The equation for the transition wave that propagates with a constant speed becomes

$$\frac{\mathrm{d}^2 u_m}{\mathrm{d}t^2} = q_{m+1}(t) - q_m(t) + P(\eta)H(-\eta) - P(\eta+1)H(-\eta-1), \tag{60}$$

where

$$P(\eta) = P_* + (1-\gamma)(q - q_*), \tag{61}$$

$\eta = m - vt$, and it is assumed that $0<v<\min(\sqrt{\gamma}, 1)$.

As in the previous case, for $\gamma = 1$, we represent the solution as the sum of an incident wave, q^0 = const, and a steady-state solution with respect to the particle velocity and elongation $q(\eta)$ induced by the forces $P(\eta)$

$$q = q_{\text{total}} = q^0 + q(\eta). \tag{62}$$

Eqs. (60) and (61) can now be rewritten in the form

$$\begin{aligned} v^2 \frac{\mathrm{d}^2 q(\eta)}{\mathrm{d}\eta^2} + 2q(\eta) - q(\eta+1) - q(\eta-1) \\ = [P_* - (1-\gamma)(q_* - q^0)][2H(-\eta) - H(-\eta+1) - H(-\eta-1)] \\ + (1-\gamma)[2q(\eta)H(-\eta) - q(\eta-1)H(-\eta+1) - q(\eta+1)H(-\eta-1)], \end{aligned}$$

$$P(\eta) = P_* + (1-\gamma)(q(\eta) + q^0 - q_*). \tag{63}$$

Fourier transform. The Fourier transform of the equation leads to

$$h(k)q_+(k) + g(k)q_-(k) = [P_* - (1-\gamma)(q_* - q^0)]\frac{2(1-\cos k)}{\mathrm{i}k}, \tag{64}$$

where

$$\begin{aligned} h(k) &= (s + \mathrm{i}kv)^2 + 2(1-\cos k), \\ g(k) &= (s + \mathrm{i}kv)^2 + 2\gamma(1-\cos k) \end{aligned} \tag{65}$$

and $s \to +0$ (here we consider the prelimiting expression $s + \mathrm{i}kv$ instead $\mathrm{i}kv$ in accordance with the above-mentioned causality principle). Further, $q_+(k)$ and $q_-(k)$ are the right-side and left-side Fourier transforms

$$\begin{aligned} q_+(k) &= \int_0^\infty q(\eta)\mathrm{e}^{\mathrm{i}k\eta}\,\mathrm{d}\eta, \\ q_-(k) &= \int_{-\infty}^0 q(\eta)\mathrm{e}^{\mathrm{i}k\eta}\,\mathrm{d}\eta. \end{aligned} \tag{66}$$

It follows from Eq. (65) that

$$2(1-\cos\,k) = \frac{h(k) - g(k)}{1-\gamma}. \tag{67}$$

Substitute this into Eq. (64), and rewrite it as

$$L(k)q_+(k) + q_-(k) = \frac{q_{**}}{\mathrm{i}k}[L(k) - 1], \tag{68}$$

where

$$L(k) = \frac{h(k)}{g(k)},$$
$$q_{**} = \frac{P_* - (1-\gamma)(q_* - q^0)}{1-\gamma}. \tag{69}$$

Note that the function $L(k)$ is estimated as $L(k) - 1 = \mathrm{O}(k^2)$ $(k \to 0)$ and hence the right-hand side of Eq. (68) is regular at $k = 0$.

Factorization of $L(k)$. To find two functions $q_\pm(k)$ from the single equation (68) we use the Wiener–Hopf technique. The first step is the factorization of $L(k)$. It should be represented as the product

$$L(k) = L_+(k)L_-(k), \tag{70}$$

where $L_+(k)$ has no zeros and singularities in the upper complex half-plane including the real axis, and $L_-(k)$ has no zeros and singularities in the lower half-plane including the real axis. The factorization can be done (for $s>0$) using the Cauchy-type integral.

Before this we normalize $L(k)$ with the goal to separate its zeros and poles in a vicinity of $k = 0$. Represent $L(k)$ as

$$L(k) = L^0(k)l(k), \tag{71}$$

where

$$l(k) = \frac{[s + \mathrm{i}(1+v)k][s - \mathrm{i}(1-v)k]}{[s + \mathrm{i}(\sqrt{\gamma}+v)k][s - \mathrm{i}(\sqrt{\gamma}-v)k]}\,\frac{\gamma - v^2}{1 - v^2}. \tag{72}$$

Note that

$$L(0) = 1, \quad l(0) = \frac{\gamma - v^2}{1 - v^2}, \quad L^0(0) = \frac{1 - v^2}{\gamma - v^2},$$
$$L(\pm\infty) = l(\pm\infty) = L^0(\pm\infty) = 1. \tag{73}$$

In addition, the index of each of the considered functions is equal to zero, for example

$$\mathrm{Ind}\, L^0(k) = \frac{1}{2\pi}[\mathrm{Arg}\, L^0(\infty) - \mathrm{Arg}\, L^0(-\infty)] = 0. \tag{74}$$

Factorization of the multiplier $l(k)$ is straightforward:

$$l(k) = l_+(k)l_-(k),$$

$$l_+(k) = \frac{s - \mathrm{i}(1-v)k}{s - \mathrm{i}(\sqrt{\gamma}-v)k}\sqrt{\frac{\gamma - v^2}{1-v^2}},$$

$$l_-(k) = \frac{s + \mathrm{i}(1+v)k}{s + \mathrm{i}(\sqrt{\gamma}+v)k}\sqrt{\frac{\gamma - v^2}{1-v^2}}. \tag{75}$$

The functions $L^0(k)$ and $\ln L^0(k)$ are regular in a vicinity of $k = 0$. The conditions at infinity in Eqs. (73) and the equality in Eq. (74) allows us to use the Cauchy-type integral for the factorization of $L^0(k)$:

$$L^0(k) = L^0_+(k)L^0_-(k),$$

$$L^0_\pm(k) = \exp\left[\pm\frac{1}{2\pi\mathrm{i}}\int_{-\infty}^{\infty}\frac{\ln L^0(\xi)}{\xi - k}\,\mathrm{d}\xi\right] \quad [\mathrm{Arg}\,L(\infty) = 0], \tag{76}$$

where $\Im k > 0$ for L_+ and $\Im k < 0$ for L_-.

We mention in addition, that when $s = 0$ there are real singular points of $\ln L^0(k)$, that correspond to the real zeros and singular points of $L^0(k)$ and, therefore, of $L(k)$. When $s > 0$, these singularities move either to the upper or the lower half-plane. Thus, for $s > 0$ functions $L^0(k)$ and $1/L^0(k)$ are regular on the real axis; functions $L^0_+(k)$ and $1/L^0_+(k)$ are regular at the half-plane $\Im k \geqslant 0$, functions $L^0_-(k)$ and $1/L^0_-(k)$ are regular at the half-plane $\Im k \leqslant 0$. When $s \to 0$, $\mathrm{Arg}\,L^0(k)$ (in contrast to $\mathrm{Arg}\,L(k)$) uniformly tends to zero in a vicinity of the origin, $k = 0$ ($\mathrm{Arg}\,L^0(0) = \mathrm{Arg}\,L(0) = 0$). Function $\mathrm{Arg}\,L^0(k)$ is odd, while $\ln|L^0(k)|$ is even.

Using these facts, we derive from Eq. (76) and (75) the following representations:

$$L^0_\pm(0) = \lim_{p\to+0} L^0(\pm\mathrm{i}p) = \sqrt{\frac{1-v^2}{\gamma - v^2}}\,\mathscr{R}^{\pm1},$$

$$L^0_\pm(\pm\infty) = 1,$$

$$L_+(k) \sim \frac{s - \mathrm{i}(1-v)k}{s - \mathrm{i}(\sqrt{\gamma}-v)k}\mathscr{R} \quad (k \to 0),$$

$$L_-(k) \sim \frac{s + \mathrm{i}(1+v)k}{s + \mathrm{i}(\sqrt{\gamma}+v)k}\frac{1}{\mathscr{R}} \quad (k \to 0),$$

$$L_\pm(0) = \mathscr{R}^{\pm1}, \quad \mathscr{R} = \exp\left[\frac{1}{\pi}\int_0^\infty \frac{\mathrm{Arg}\,L^0(\xi)}{\xi}\,\mathrm{d}\xi\right],$$

$$L_\pm(\pm\mathrm{i}\infty) = l_\pm(\pm\infty) = \left(\frac{(\sqrt{\gamma}+v)(1-v)}{(\sqrt{\gamma}-v)(1+v)}\right)^{\pm1/2}. \tag{77}$$

Here, the first multiplier in the expression for $L^0_\pm(0)$ is defined by a half-residue at $k = 0$.

Assume that $s = +0$ and let us number the increasing positive zeros of $h(k)$ as $h_1 < h_2 < \cdots < h_{2l+1}$ and similarly, the increasing positive zeros of $g(k)$ as $g_1 < g_2 < \cdots < g_{2d+1}$. The transition front speed, v, is assumed such that the zeros

are simple (of the first order) and the corresponding functions change their signs when they pass the root.

From expressions (65), we determine arguments of $h(k)$ and $g(k)$:

$$\begin{aligned}&\operatorname{Arg} h(k)=0 \quad (h_{2v}<k<h_{2v+1}), \quad \operatorname{Arg} h(k)=\pi \quad (h_{2v+1}<k<h_{2v+2}),\\ &v=0,1,\dots,l, \quad h_0=0, \quad h_{2l+2}=\infty,\\ &\operatorname{Arg} g(k)=0 \quad (g_{2v}<k<g_{2v+1}), \quad \operatorname{Arg} g(k)=\pi \quad (g_{2v+1}<k<g_{2v+2}),\\ &v=0,1,\dots,d; \quad g_0=0, \quad g_{2d+2}=\infty. \end{aligned} \tag{78}$$

Finally, function $\mathscr{R}$ can thus be expressed in terms of the real zeros of $h(k)$ and $g(k)$ as

$$\mathscr{R}=\frac{h_2h_4\dots h_{2l}\, g_1g_3\dots g_{2d+1}}{h_1h_3\dots h_{2l+1}\, g_2g_4\dots g_{2d}}. \tag{79}$$

Wiener–Hopf equation. The Wiener–Hopf equation (68) can now be written as

$$L_+(k)q_+(k)+\frac{q_-(k)}{L_-(k)}=\frac{q_{**}}{\mathrm{i}k}\left[L_+(k)-\frac{1}{L_-(k)}\right], \tag{80}$$

where $k=0$ is still a regular point of the right-hand side. Next we rewrite this equation in the identical form

$$L_+(k)q_+(k)+\frac{q_-(k)}{L_-(k)}=q_{**}\left\{\frac{L_+(k)-\mathscr{R}}{\mathrm{i}k}-\left[\frac{1}{L_-(k)}-\mathscr{R}\right]\frac{1}{\mathrm{i}k}\right\}, \tag{81}$$

where $k=0$ is a regular point for both terms on the right-hand side.

Solution. We now obtain the solution to Eq. (81) as

$$\begin{aligned}&q_+(k)=\frac{q_{**}}{\mathrm{i}k}\left[1-\frac{\mathscr{R}}{L_+(k)}\right],\\ &q_-(k)=-\frac{q_{**}}{\mathrm{i}k}[1-\mathscr{R}L_-(k)].\end{aligned} \tag{82}$$

In particular, we find from these formulas and from Eqs. (77), the following representations:

$$\begin{aligned}&q(0)=q^0+\lim_{k\to\mathrm{i}\infty}(-\mathrm{i}k)[q_+(k)=q^0+\lim_{k\to-\mathrm{i}\infty}(\mathrm{i}k)q_-(k)\\ &\quad=q^0-q_{**}(1-\mathscr{R}_*)=\mathscr{R}_*q^0-(1-\mathscr{R}_*)\left(\frac{P_*}{1-\gamma}-q_*\right),\\ &\mathscr{R}_*=\mathscr{R}\sqrt{\frac{(\sqrt{\gamma}-v)(1+v)}{(\sqrt{\gamma}+v)(1-v)}}.\end{aligned} \tag{83}$$

Using condition (18) of the transition we now find the incident wave as

$$q^0=q_*+\frac{P_*}{1-\gamma}\left(\frac{1}{\mathscr{R}_*}-1\right). \tag{84}$$

The uniform part of the strain, as the contribution of singular points approaching zero with $s\to 0$, is

$$q = q^+ = q^0 - \frac{q_{**}(1-\sqrt{\gamma})}{1-v} = q_* - \frac{P_*}{1-\gamma}\left(1 - \sqrt{\frac{\gamma - v^2}{1-v^2}}\,\frac{1}{\mathscr{R}}\right) \quad (\eta > 0),$$

$$q = q^- = q^0 + \frac{q_{**}(1-\sqrt{\gamma})}{\sqrt{\gamma}+v} = q_* - \frac{P_*}{1-\gamma}\left(1 - \sqrt{\frac{1-v^2}{\gamma - v^2}}\,\frac{1}{\mathscr{R}}\right) \quad (\eta < 0). \tag{85}$$

At $\eta > 0$ the corresponding nondimensional particle velocity, by its value, is equal to $-q$ since it corresponds to a free wave propagating to the right with the unit speed. To find the uniform part of the particle velocity at $\eta < 0$ we use the momentum conservation law for the *original* problem where there are no external forces at $\eta < 0$

$$\left(\frac{\mathrm{d}u}{\mathrm{d}t}\right)^- - \left(\frac{\mathrm{d}u}{\mathrm{d}t}\right)^+ = -\frac{1}{v}\left(T^- - T^+\right) \tag{86}$$

with

$$T^+ = q^+ \quad (\eta > 0),$$
$$T^- = q^- - P_* - (1-\gamma)(q^- - q_*) \quad (\eta < 0), \tag{87}$$

where the superscripts $\pm$ are used to indicate the uniform parts of the values at $\eta > 0$ and $\eta < 0$, respectively. As a result we find

$$\left(\frac{\mathrm{d}u}{\mathrm{d}t}\right)^+ = -q_* + \frac{P_*}{1-\gamma}\left(1 - \sqrt{\frac{\gamma - v^2}{1-v^2}}\,\frac{1}{\mathscr{R}}\right),$$

$$\left(\frac{\mathrm{d}u}{\mathrm{d}t}\right)^- = \left(\frac{\mathrm{d}u}{\mathrm{d}t}\right)^+ - \frac{P_* v}{\mathscr{R}\sqrt{(\gamma - v^2)(1-v^2)}}$$

$$= -q_* - \frac{P_*}{1-\gamma}\left(\sqrt{\frac{1-v^2}{\gamma - v^2}}\,\frac{\gamma + v}{1+v}\,\frac{1}{\mathscr{R}} - 1\right). \tag{88}$$

The limit at $\gamma = 1$. To find the limits of the uniform strains (85) and particle velocities (88) we first have to find the corresponding asymptote of $\mathscr{R}$. If $\gamma \to 1$ then $g_v \to h_v$ and

$$g(g_v) = h(g_v) - (1-\gamma)2(1 - \cos g_v) = 0,$$
$$\frac{\mathrm{d}h(h_v)}{\mathrm{d}k}(g_v - h_v) \sim 2(1-\gamma)(1 - \cos h_v),$$
$$\frac{g_v}{h_v} \sim 1 + \frac{(1-\gamma)h_v v^2}{2(\sin h_v - h_v v^2)} \tag{89}$$

and referring to Eq. (79)

$$\frac{1}{\mathscr{R}} \sim 1 - (1-\gamma)\sum_{v=0}^{n}\left(Q_{2v+1} - Q_{2v}\right). \tag{90}$$

It can now be seen that in the limit, $\gamma \to 1$, expressions (85) and (88) lead to those for the parallel-branch cases (42) and (45).

The force–speed relation. Relations between the speed, v, and the applied force, $\mathscr{P}$, or the speed and a given particle velocity, $-w$, follows from Eqs. (87), (85) and (88) as

$$\frac{P_*}{1-\gamma}\left(\sqrt{\frac{1-v^2}{\gamma-v^2}}\,\frac{\gamma}{\mathscr{R}}-1\right)=\mathscr{P}-q_*,$$

$$\frac{P_*}{1-\gamma}\left(\sqrt{\frac{1-v^2}{\gamma-v^2}}\,\frac{\gamma+v}{1+v}\,\frac{1}{\mathscr{R}}-1\right)=w-q_*. \tag{91}$$

The nondimensional values (47) can now be used to decrease the number of parameters in these equations. Recall that this is achieved by means of division by q_*. The $\mathscr{P}--v$ relations for $P_*=q_*$, $\gamma=\frac{1}{2}$ and $\gamma=2$ are presented in Fig. 11.

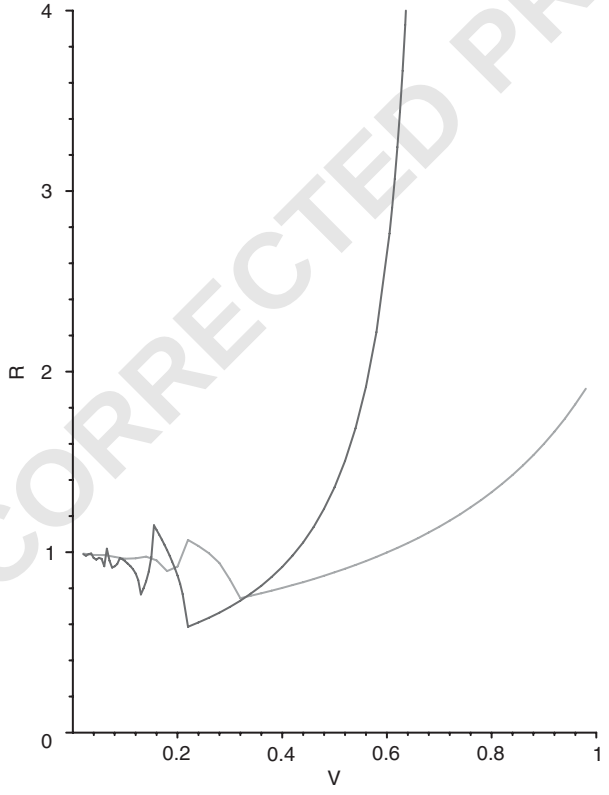

Fig. 11. The force–speed dependence for $P_*=\mu q_*$. Here $V=v/c$ and $R=\mathscr{P}/P_*$. The lower curve ($R=2$ at $V=1$) corresponds to $\gamma=2$, the upper curve ($R\to\infty$ when $V\to\sqrt{5}$) corresponds to $\gamma=\frac{1}{2}$.

3.2. Sinusoidal waves and dissipation

As follows from the solution in Eq. (82) the oscillating waves corresponding to wavenumbers h_{2v} carry energy from the transition front to $+\infty$ since the group velocity at $k = h_{2v}$ is greater than the phase velocity v. The waves corresponding to wavenumbers g_{2v+1} carry energy to $-\infty$, these waves are present behind the transition front because they correspond to the opposite relation between the group and phase velocities, see Fig. 4. The amplitudes of the sinusoidal waves can be determined in the same way as in the case $P_* = (1-\gamma)q_*$ considered in Slepyan and Troyankina, 1984 (also see Slepyan, 2002) using a different type of the factorization. The total dissipation due to the existence of the oscillating waves can be calculated as in the considered above parallel-branch case using the dependence presented in Fig. 2(c). The energy dissipation rate per unit time is

$$D = \frac{v}{2}[(T^- + T^+)(q^- - q^+) - (q^+ + q_*)(q_* - q^+) - (q_* - P_* + T^-)(q^- - q_*)]. \tag{92}$$

Recall the values with the upper sign $\pm$ correspond to the uniform parts of those at $\eta > 0$ and $\eta < 0$, respectively. Using the obtained above expressions for the values in Eq. (92) it can be found that

$$D = \frac{P_*^2 v}{2(1-\gamma)}\left(\frac{1}{\mathscr{R}^2} - 1\right). \tag{93}$$

At the same time, the total energy flux is

$$N = T^- w. \tag{94}$$

4. Conclusions

1. In this paper, especially in Part I, it is demonstrated that a properly designed bistable structure being under an impact can absorb an increased amount of energy. This is achieved by means of the large strain delocalization and by the transfer of a considerable part of the input energy (for example, the kinetic energy of the hammering mass) into the energy of high-frequency oscillations. The bistable structure role is just the delocalization and transformation of the nonoscillating wave energy into the oscillating one. In Part I of the paper, the stress–strain dependence with a gap between two branches of the resistance is considered. General considerations, numerical simulations and analytical estimations are presented for quasi-static and dynamic extension of the chain to elucidate the role of the bistability and especially the role of the gap in the energy consumption; an optimal value of the gap is found. In Part II, the same bistable-bond chain is considered, but without the gap. This simplification allowed us to obtain analytical solutions for an arbitrary

relation between the branch modules. The analytical treatment of the problem represents the main contents of this Part.

2. For the energy consumption in an elastic bistable structure the constraint is that the strength of the second branch, $T(q_{**}-0)$, must be large enough to withstand the dynamic overshoot caused by the sudden breaks of the basic links, that is, the waiting links must withstand both the nonoscillating and oscillating waves. Note, however, that the overshoot can be suppressed by internal inelastic resistances which speed up the energy transfer from the mechanical oscillations to heat (see Slepyan, 2000, 2002). In this sense, the nonoscillating wave amplitudes are critical, and the energy transfer to the oscillating waves that decreases the nonoscillating wave amplitudes is fruitful.

3. Mathematically, two cases are different: parallel-branch diagram, $\gamma=1$, and nonparallel one, $\gamma\neq1$. Although the former follows from the latter as a limit, the mathematical difference reflects different physics. In the parallel-branch case, there exist pure resonances which correspond to a hypothetic situation where the transition front speed and hence the wave phase velocity coincide with the group velocity. In this case, there is no energy flux (for this resonant wave) from the transition front, and the wave amplitude increases in time. The steady-state solution does not exist at this speed. In contrast, in the case of different modules, if the speed corresponds to a resonant wave for a one branch, it does not correspond to such a wave for the other, and the latter represents a nonresonant waveguide for the energy. As a result, there is no pure resonance speeds in this nonparallel case.

4. In this paper, a mechanical problem is considered, mainly as how the bistability increases the energy consumption in the chain. At the same time, the formulations and the results may have an interest in different fields, in particular, we can note waves of instability or crushing waves in an extended structure, or a material phase transition where the bistability or multistability plays a crucial role. In this Part, we refer to some phase transition papers where this model is exploited.

5. Uncited references

Charlotte and Truskinovsky (2002); Kresse and Truskinovsky (2003, 2004).

Acknowledgements

This research was supported by The Israel Science Foundation, Grants No. 28/00-3 and No. 1155/04, ARO Grant No. 41363-MA, and NSF Grant No. DMS-0072717.

References

Balk, A.M., Cherkaev, A.V., Slepyan, L.I., 2001a. Dynamics of chains with non-monotone stress–strain relations. I. Model and numerical experiments. J. Mech. Phys. Solids 49, 131–148.

Balk, A.M., Cherkaev, A.V., Slepyan, L.I., 2001b. Dynamics of chains with non-monotone stress–strain relations. II. Nonlinear waves and waves of phase transition. J. Mech. Phys. Solids 49, 149–171.

Bolotovsky, B.M., Stolyarov, S.N., 1972. On radiation principles for a medium with dispersion. In: Problems for Theoretical Physics. Nauka, Moscow, pp. 267–280 (in Russian).

Charlotte, M., Truskinovsky, L., 2002. Linear chains with a hyper-pre-stress. J. Mech. Phys. Solids 50, 217–251.

Fedelich, B., Zanzotto, G., 1992. Hysteresis in discrete systems of possibly interacting elements with a double-well energy. J. Nonlinear Sci. 2, 319–342.

Frenkel, J., Kontorova, T., 1938. On the theory of plastic deformation and twinning. Sov. Phys. JETP 13, 1–10.

Kresse, O., Truskinovsky, L., 2003. Mobility of lattice defects: discrete and continuum approaches. J. Mech. Phys. Solids 51 (7), 1305–1332.

Kresse, O., Truskinovsky, L., 2004. Lattice friction for crystalline defects: from dislocations to cracks, submitted for publication.

Marder, M., Gross, S., 1995. Origin of crack tip instabilities. J. Mech. Phys. Solids 43, 1–48.

Muller, I., Villaggio, P., 1977. A model for an elastoplastic body. Arch. Rat. Mech. Anal. 65, 25–46.

Ngan, S.-C., Truskinovsky, L., 1999. Thermal trapping and kinetics of martensitic phase boundaries. J. Mech. Phys. Solids 47, 141–172.

Ngan, S.-C., Truskinovsky, L., 2002. Thermo-elastic aspects of dynamic nucleation. J. Mech. Phys. Solids 50, 1193–1229.

Puglisi, G., Truskinovsky, L., 2000. Mechanics of a discrete chain with bi-stable elements. J. Mech. Phys. Solids 48, 1–27.

Puglisi, G., Truskinovsky, L., 2002a. Rate-independent hysteresis in a bi-stable chain. J. Mech. Phys. Solids 50, 165–187.

Puglisi, G., Truskinovsky, L., 2002b. A model of transformational plasticity. Cont. Mech. Therm. 14, 437–457.

Rogers, R.C., Truskinovsky, L., 1997. Discretization and hysteresis. Physica B 233, 370–375.

Slepyan, L.I., 2000. Dynamic factor in impact, phase transition and fracture. J. Mech. Phys. Solids 48, 931–964.

Slepyan, L.I., 2001. Feeding and dissipative waves in fracture and phase transition. II. Phase-transition waves. J. Mech. Phys. Solids 49, 513–550.

Slepyan, L.I., 2002. Models and Phenomena in Fracture Mechanics. Springer, Berlin.

Slepyan, L.I., Troyankina, L.V., 1984. Fracture wave in a chain structure. J. Appl. Mech. Techn. Phys. 25 (6), 921–927.

Slepyan, L.I., Troyankina, L.V., 1988. Impact waves in a nonlinear chain. In: Strength and Visco-plasticity. Nauka, Moscow, pp. 301–305 (in Russian).

Truskinovsky, L., Vainchtein, A., 2004a. The origin of the nucleation peak in transformational plasticity. J. Mech. Phys. Solids 52, 1421–1446.

Truskinovsky, L., Vainchtein, A., 2004b. Explicit kinetic relation from "first principles". In: Ogden, R., Gao, D. (Eds.), Mechanics of Material forces, Euromech 445, Advances in Mechanics and Mathematics. Kluwer, Dordrecht, pp. 1–8 (in press).